Research Article

ANALYSIS OF A BOUNDARY LAYER FLOW OF A NANOFLUID OVER AN INCLINED PLANE VIA ADM

Gbolahan BOLARIN*[1], Abdulhakeem YUSUF[2], Samson Temitope ADEKUNLE[3], Yomi Monday AIYESIMI[4], Mohammed JIYA[5]

[1]*Department of Mathematics, Federal University of Technology, PMB 65, Minna, 00176-0000 Nigeria, Niger State, NIGERIA;* ORCID: 0000-0002-7026-252X
[2]*Department of Mathematics, Federal University of Technology, PMB 65, Minna, 00176-0000 Nigeria, Niger State, NIGERIA;* ORCID: 0000-0002-9238-6283
[3]*Department of Mathematics, Federal University of Technology, PMB 65, Minna, 00176-0000 Nigeria, Niger State, NIGERIA;* ORCID: 0000-0003-4828-6039
[4]*Department of Mathematics, Federal University of Technology, PMB 65, Minna, 00176-0000 Nigeria, Niger State, NIGERIA;* ORCID: 0000-0003-4586-450X
[5]*Department of Mathematics, The University of Gambia, GAMBIA;* ORCID: 0000-0002-7089-6283

ABSTRACT

The study of Boundary layer flow of a nanofluid in an inclined moving plane at an angle Θ is carried out analytically using Adomian decomposition method (ADM). The Mathematical equations presented incorporate the effects of Brownian motion, thermophoresis and Magnetic parameter. Unlike the previously published works which considered a convective heating boundary condition. The present study considered an inclined moving plane at angle Θ in 2-dimensions with thermal conditions of constant temperature and heat flux. The solutions to the momentum, temperature and concentration distributions were obtained via the ADM and depends on, Magnetic parameter M, Prandtl number Pr, Lewis number Le, the Brownian motion parameter Nb, the thermophoresis parameter Nt and Grashof numbers Gr and Gc. A good agreement was established between the Adomian Decomposition method and the Numerical method (Shooting technique) for some values of M while other Physical terms on the velocity profile are set to 0. Results are presented in graphical forms illustrating the effects of these parameters on Momentum, thermal and concentration boundary layers. The momentum boundary layer reduces with increase in the magnetic parameter.
Keywords: Adomian decomposition method (ADM), nanofluid, boundary layers, inclined plane and hydromagnetic.

1. INTRODUCTION

The importance of fluid flow over a moving surface in applications like extrusion, wire drawing, metal spinning, hot rolling can never be over emphasis. It is crucial to understand the heat and flow characteristics of the process so that the finished product meets the desired quality specifications (Altan *et al.;* 1979). A wide v ariety of problems dealing with heat and fluid flow

---

* Corresponding Author: e-mail: g.bolarin@futminna.edu.ng, tel: 2348033883137

over a stretching sheet have been studied with both Newtonian and non-Newtonian fluids and with the inclusion of imposed electric and magnetic fields, different thermal boundary conditions, and power law variation of the stretching velocity. Both similarities as well as direct numerical solutions of the convective transport equations have been reported. A representative sample of the recent literature on the topic is provided by reference (Prasad *et al.*, 2010).

The stagnation flow for a nanofluid over a stretching sheet was studied by Mustafa *et al.* (2011) analytically. Rashidi *et al.* (2014) compared the two phases and single phase of heat transfer and flow field of copper-water nanofluid in a wavy channel numerically. Beg *et al.* (2014) presented a comparative numerical solution for both single and two-phase models for Bio-Nano-fluid transport phenomena. Makinde and Aziz (2011), carried the study of boundary layer flow of a nanofluid past a stretching sheet with a convective boundary condition using Numerical approach and Abu-Nada *et al.* (2010) illustrated the impacts of variable properties in natural convection nanofluid flow. Rashidi *et al.* (2013) showed how the second law of thermodynamics can be applied to MHD incompressible nanofluid flow over a porous rotating disk. Yusuf *et al.* (2016) presented analytical solution of a nanofluid in an inclined permeable wavy channel unsteady with Soret and Duffour effects using the Adomian Decomposition Method. Recently, Yusuf *et al.* (2018) considered Boundary layer flow of a nanofluid in an inclined wavy wall with convective boundary condition. The problem was solved at $Lx = \dfrac{\pi}{2}$ (Where *Lx* is a point on the wavy wall) and a flow back was observed in the region closed to the wavy wall.

Ayub *et. al* (2016) considered boundary layer flow of nanofluid that is electrically conducting over a Riga plate. The numerical model fuses the Brownian motion and the thermophoresis impacts because of the nanofluid and the Grinberg term for the wall parallel Lorentz force due to the Riga plate in the presence of slip effects. Bahtti *et al* (2016) describes the combine effects of thermo-diffusion and thermal radiation on Williamson nanofluid over a porous stretching sheet. Similarity transformation variables have been used to model the governing equations of momentum, energy, solute, and nanoparticle concentration. Successive linearization method (SLM) and Chebyshev spectral collocation method (CSC) are applied to solve the resulting coupled ordinary nonlinear differential equations. The numerical comparison has also presented for skin friction coefficient and local Nusselt number as a special case. Qing *et al.*(2016), investigate entropy generation on MHD Casson nanofluid over a porous Stretching/Shrinking surface. The influences of nonlinear thermal radiation and chemical reaction were also taken into account. They established that concentration profile decreases for higher values of chemical reaction parameter and Brownian motion parameter but its behaviours seem to be opposite for thermophoresis parameter increases. Bhatti *et al* (2018) carried out analysis of stagnation point flow over a permeable shrinking sheet under the influence of Magnetohydrodynamics (MHD) using Successive linearization method. The governing equations are simplified with the help of similarity variables. The impacts of various pertinent parameters are demonstrated numerically and graphically. It was found that the present methodology converges more rapidly. Hassan *et al* (2018), presented a study which deals with the PVA solution-based non-Newtonian Al2O3-m nanofluid flow along with heat transfer over wedge. It was noticed that resistance between adjacent layers of moving fluid is enhanced due to these nanoparticles which leads to decline in velocity profile and increases in shear stress at wall.

To the best of our knowledge, this work, analysis of a boundary layer flow of a nanofluid over an inclined plane via ADM is new in the literature.

2. PROBLEM FORMULATION

Considering 2-dimensional steady nanofluid flow in a moving plane, inclined at angle Θ. The flow is along *y=0* and at this point the wall velocity is assumed to be *ax,* temperature and concentration are constant, ie Tw and Cw respectively. The velocity is 0 and the temperature and

concentration are T_∞ and C_∞ at larger values of y ($y \to \infty$). Following the work of Yusuf *et al.*(2019), the 2-dimensional steady state is governed by the following:
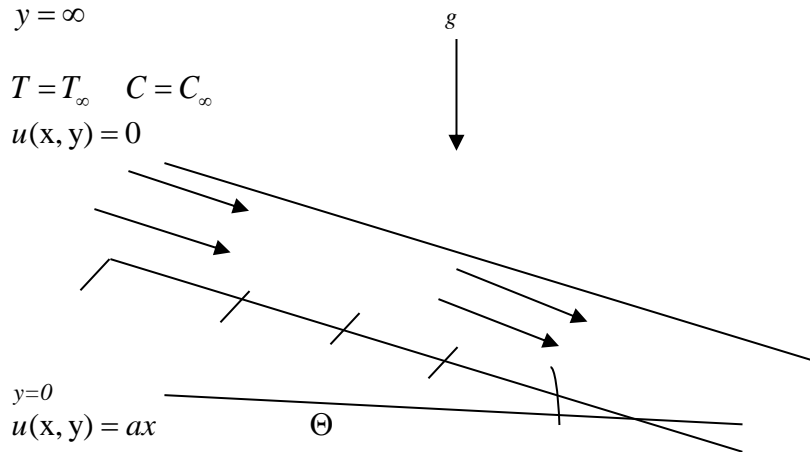
$y = \infty$

g

$T = T_\infty \quad C = C_\infty$
$u(\mathrm{x}, \mathrm{y}) = 0$

y=0
$u(\mathrm{x}, \mathrm{y}) = ax$

Θ

Figure 1. Diagram Showing the Flow Model

$T=Tw \quad C=Cw$

Continuity equation:

$$\frac{\partial u}{\partial x} + \frac{\partial v}{\partial y} = 0 \tag{1}$$

Momentum equation:

$$u\frac{\partial u}{\partial x} + v\frac{\partial u}{\partial y} = \upsilon\left(\frac{\partial^2 u}{\partial x^2} + \frac{\partial^2 u}{\partial y^2}\right) - \frac{\sigma B_0^2}{\rho}u + g\beta(T - T_\infty)\mathrm{Sin}\,\Theta + g\beta(C - C_\infty)\mathrm{Sin}\,\Theta \tag{2}$$

Energy equation:

$$u\frac{\partial T}{\partial x} + v\frac{\partial T}{\partial y} = \alpha(\frac{\partial^2 T}{\partial x^2} + \frac{\partial^2 T}{\partial y^2}) + \tau\left(D_B(\frac{\partial C}{\partial x}\frac{\partial T}{\partial x} + \frac{\partial C}{\partial y}\frac{\partial T}{\partial y}) + \frac{D_T}{T_\infty}\left(\left(\frac{\partial T}{\partial x}\right)^2 + \left(\frac{\partial T}{\partial y}\right)^2\right)\right) \tag{3}$$

Nanofraction equation:

$$u\frac{\partial C}{\partial x} + v\frac{\partial C}{\partial y} = D_B\left(\frac{\partial^2 C}{\partial x^2} + \frac{\partial^2 C}{\partial y^2}\right) + \left(\frac{D_T}{T_\infty}\right)\left(\frac{\partial^2 T}{\partial x^2} + \frac{\partial^2 T}{\partial y^2}\right) \tag{4}$$

Subject to the boundary conditions:

$$\left.\begin{array}{l} y = 0: \quad u = ax, \quad v = 0, \ T = T_W, \quad C = C_W, \\ y \to \infty: \quad u \to 0, \qquad T \to T_\infty, \qquad C \to C_\infty, \end{array}\right\} \tag{5}$$

Nomenclature

x and y are fluid distances

u velocities along x

v velocities along y

B_0 external magnetic field at constant pressure

D_B Brownian diffusion coefficient diffusion coefficient

$\tau = \dfrac{(\rho c)_p}{(\rho c)_f}$ ratio between the effective heat

g acceleration due to gravity

β volumetric coefficient of thermal expansion distance

$f(\eta)$ dimensionless fluid velocity temperature

$\phi(\eta)$ dimensionless fluid concentration

number $Gr_C = \dfrac{g\beta_1 (C_W - C_\infty)}{av}$ Concentration Grashof number

Magnetic parameter

$Le = \dfrac{v}{D_B}$ Lewis Number

$N_b = \dfrac{(\rho c)_p D_B (C_W - C_\infty)}{(\rho c)_f v}$

$N_t = \dfrac{(\rho c)_p D_T (T_W - T_\infty)}{(\rho c)_f T_\infty v}$ Thermopheris parameter

α thermal diffusivity

v kinematic viscousity

C_p specific heat capacity

D_T is the thermopheric

ρ density,

σ electrical conductivity

η dimensionless fluid

$\theta(\eta)$ dimensionless fluid

$Gr_T = \dfrac{g\beta_1 (T_W - T_\infty)}{av}$ Thermal grashof

$M = \dfrac{\sigma B_0^{\,2}}{a\rho}$

$\Pr = \dfrac{v}{\alpha}$ Prandtl number

Brownian diffusion

From the following dimensionless variables:-

$$\eta = \sqrt{\frac{a}{v}}\, y \,,\ \ \psi = \sqrt{av}\, x f(\eta) \ \ \theta(\eta) = \frac{T - T_\infty}{T_W - T_\infty} \,,\ \text{and} \ \ \phi(\eta) = \frac{C - C_\infty}{C_W - C_\infty} \quad,\ \text{we}$$

have that

$$\frac{\partial \eta}{\partial y} = \sqrt{\frac{a}{\upsilon}}, \frac{\partial \eta}{\partial x} = 0, \quad \frac{\partial \psi}{\partial f} = (a\upsilon)^{\frac{1}{2}} x$$

$$u = \frac{\partial \psi}{\partial y} \equiv \frac{\partial \psi}{\partial f} \frac{\partial \eta}{\partial y} \frac{\partial f}{\partial \eta} = axf'(\eta)$$

$$v = -\frac{\partial \psi}{\partial x} = -\sqrt{a\upsilon} f(\eta)$$

$$\frac{\partial u}{\partial y} = \frac{\partial}{\partial y} \left(\frac{\partial \psi}{\partial y} \right) = \frac{\partial \eta}{\partial y} \frac{\partial}{\partial \eta} \left(axf'(\eta) \right) = \sqrt{\frac{a}{\upsilon}} axf''(\eta)$$

$$\frac{\partial u}{\partial x} = \frac{\partial}{\partial x} \left(\frac{\partial \psi}{\partial y} \right) = \frac{\partial}{\partial x} \left(axf'(\eta) \right) = af'(\eta)$$

$$v \frac{\partial u}{\partial y} = -a^2 xf(\eta) f''(\eta)$$

$$u \frac{\partial u}{\partial x} = a^2 xf'^2(\eta)$$

$$\frac{\partial^2 u}{\partial x^2} = \frac{\partial^2}{\partial x^2} \left(\frac{\partial \psi}{\partial y} \right) = 0$$

$$\frac{\partial^2 u}{\partial y^2} = \frac{\partial^2}{\partial y^2} \left(\frac{\partial \psi}{\partial y} \right) = \frac{\partial \eta}{\partial y} \frac{\partial}{\partial \eta} \left(\sqrt{\frac{a}{\upsilon}} axf''(\eta) \right) = \frac{a^2 xf'''(\eta)}{\upsilon}$$

$$Let \ \beta = \beta(x) = \frac{\beta_1 ax}{\upsilon}$$

(6)

$$T = T_\infty + (T_W - T_\infty)\theta(\eta)$$

$$C = C_\infty + (C_W - C_\infty)\phi(\eta)$$

$$\frac{\partial T}{\partial y} = (T_W - T_\infty)\frac{\partial \eta}{\partial y}\frac{\partial \theta}{\partial \eta} = \sqrt{\frac{a}{\upsilon}}(T_W - T_\infty)\theta'(\eta)$$

$$\frac{\partial^2 T}{\partial y^2} = \frac{\partial}{\partial y}\left(\frac{\partial T}{\partial y}\right) = (T_W - T_\infty)\left(\frac{\partial \eta}{\partial y}\right)^2\frac{\partial^2 \theta}{\partial \eta^2} = \frac{a}{\upsilon}(T_W - T_\infty)\theta''(\eta)$$

$$\frac{\partial C}{\partial y} = \sqrt{\frac{a}{\upsilon}}(C_W - C_\infty)\phi'(\eta)$$

$$\frac{\partial^2 C}{\partial y^2} = \frac{a}{\upsilon}(C_W - C_\infty)\phi''(\eta)$$

$$\frac{\partial T}{\partial x} = (T_W - T_\infty)\frac{\partial \eta}{\partial x}\frac{\partial \theta}{\partial \eta} = 0$$

$$\frac{\partial^2 T}{\partial x^2} = 0$$

$$\frac{\partial C}{\partial x} = 0, \frac{\partial^2 C}{\partial x^2} = 0$$

(7)

Introducing equation (6) and (7) into equations (1) to (5), the equation reduced to the following local similarity solution:-

$$f''' + ff'' - f'^2 - Mf' + Gr_T\theta(\eta)Sin\Theta + Gr_C\phi(\eta)Sin\Theta = 0$$

$$\theta'' + \Pr f\theta' + \Pr N_b\phi'\theta' + \Pr N_t\theta'^2 = 0$$

(8)

$$\phi'' + Lef\phi' + \frac{Nt}{Nb}\theta'' = 0$$

with corresponding boundary conditions:

$$f(0) = 0, f'(0) = 1, \quad \theta(0) = 1, \quad \phi(0) = 1, \ \eta{=}0$$

(9)

$$f(\infty) = 0, \quad \theta(\infty) = 0, \quad \phi(\infty) = 0, \ \eta \to \infty$$

3. ANALYTICAL SOLUTION VIA ADM

By ADM, equation (8) can be written as

$$f(\eta) = \eta + \frac{\eta^2}{2}\alpha + L_2^{-1}\left[-ff'' + f'^2 + Mf' - Gr_T\theta(\eta)Sin\Theta - Gr_C\phi(\eta)Sin\Theta\right]$$

$$\theta(\eta) = 1 + \eta\beta + L_1^{-1}\left[-\Pr f\theta' - \Pr N_b\phi'\theta' - \Pr N_t\theta'^2\right]$$

$$\phi(\eta) = 1 + \eta\gamma + L_1^{-1}\left[-Lef\phi' - \frac{Nt}{Nb}\theta''\right]$$

$$where \quad \alpha = f''(0), \beta = \theta'(0) \text{ and } \gamma = \phi'(0)$$

$$(10)$$

Where $L_2^{-1} = \iiint[\bullet]d\eta d\eta d\eta$ and $L_1^{-1} = \iint[\bullet]d\eta d\eta$

Decomposing the dependent variables in (10) by introducing the Adomian polynomials, we have

$$\sum_{n=0}^{\infty} f_n = \eta + \frac{\eta^2}{2}\alpha + L_2^{-1}\left[-\sum_{m=0}^{\infty} A_m + \sum_{m=0}^{\infty} B_m + M\sum_{m=0}^{\infty} f_m' - Gr_T\sum_{m=0}^{\infty}\theta_m Sin\Theta - Gr_C\sum_{m=0}^{\infty}\phi_m Sin\Theta\right]$$

$$\sum_{n=0}^{\infty} \theta_n = 1 + \eta\beta + L_1^{-1}\left[-\Pr\sum_{m=0}^{\infty} C_m - \Pr N_b\sum_{m=0}^{\infty} E_m - \Pr N_t\sum_{m=0}^{\infty} F_m\right]$$

$$\sum_{n=0}^{\infty} \phi_n = 1 + \eta\gamma + L_1^{-1}\left[-Le\sum_{m=0}^{\infty} G_m - \frac{Nt}{Nb}\sum_{m=0}^{\infty}\theta_m''\right]$$

(11)

Where $A_m = f_{n-k}'f_k''$, $B_m = f_{n-k}'f_k'$, $C_m = f_{n-k}\phi_k'$, $E_m = \theta_{n-k}'\phi_k'$, $F_m = \theta_{n-k}'\theta_k'$ and $G_m = f_{n-k}\phi_k'$, Therefore,

$$f_{n+1} = L_2^{-1}\left[-\sum_{k=0}^{n} f_{n-k} f_k^{//} + \sum_{k=0}^{n} f_{n-k}^{/} f_k^{/} + Mf_n - Gr_T \theta_n Sin\Theta - Gr_C \phi_n Sin\Theta\right]$$

$$\theta_{n+1} = L_1^{-1}\left[-Pr\sum_{k=0}^{n} f_{n-k}\theta_k^{/} - Pr\,N_b\sum_{k=0}^{n}\phi_{n-k}^{/}\theta_k^{/} - Pr\,N_t\sum_{k=0}^{n}\theta_{n-k}^{/}\theta_k^{/}\right] \qquad (12)$$

$$\phi_{n+1} = L_1^{-1}\left[-Le\sum_{k=0}^{n} f_{n-k}\phi_k^{/} - \frac{Nt}{Nb}\theta_n\right]$$

Where $f_0 = \alpha e^{-\eta}$, $\theta_0 = \beta e^{-\eta}$ and $\phi_0 = \gamma e^{-\eta}$, and Maple 18 were used to compute the integrals.

4. RESULTS AND DISCUSSION

The nonlinear coupled ordinary differential equation in (8) with boundary condition (9) has been solved using the improved ADM as showed above. Maple 18 was used to obtain the integrals and the skin friction has been compared with that of Numerical for different values of Magnetic parameter as showed below in Table 1. The values of the auxiliary constants α, β and γ are obtained by invoking the initial conditions in other for the boundary conditions to be satisfied and the graphical variation of the physical properties are presented below.

Figures 2 presents the effects of magnetic parameter on velocity profile (a), temperature profile (b) and concentration (c). The fluid velocity dropped for higher values of magnetic parameter due the drag like force while temperature and concentration thickens for higher values magnetic parameter. As the magnetic parameter increases, the rate at which the concentration profile thickens becomes low as showed in Figure 2(c).
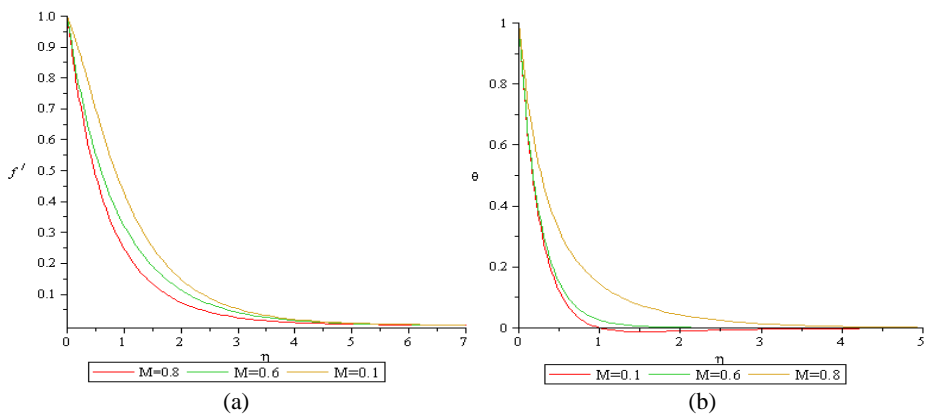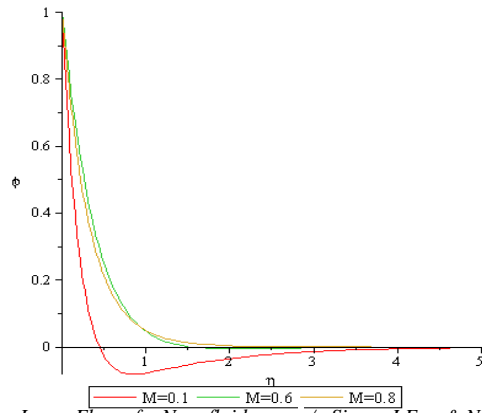
(a)

(b)

(c)

Figure 2. variation of magnetic parameter on Velocity, temperature and concentration profile
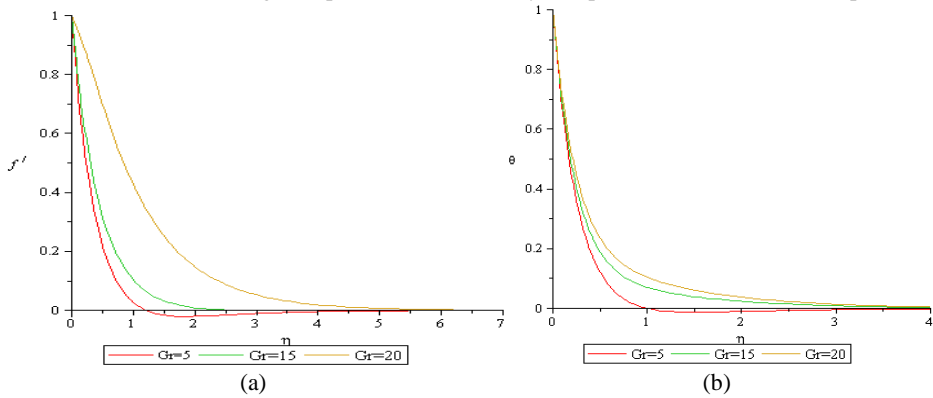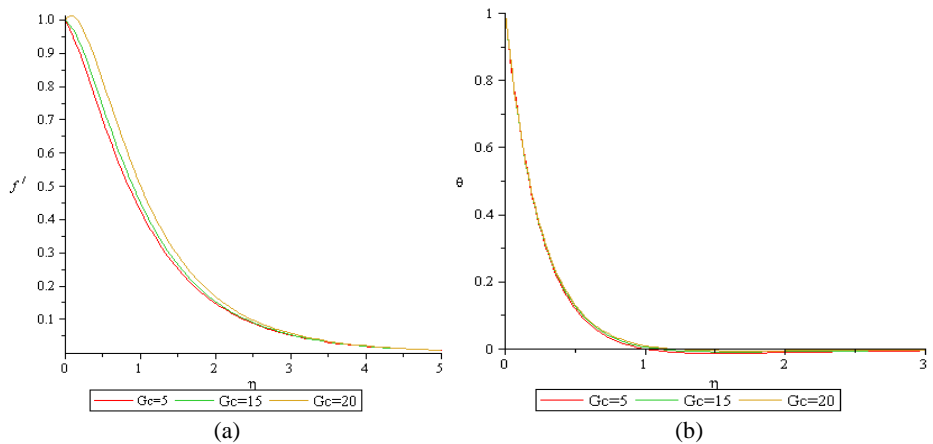

(a)

(b)

Figure 3. Variation of Thermal Grashof number on Velocity and temperature profile
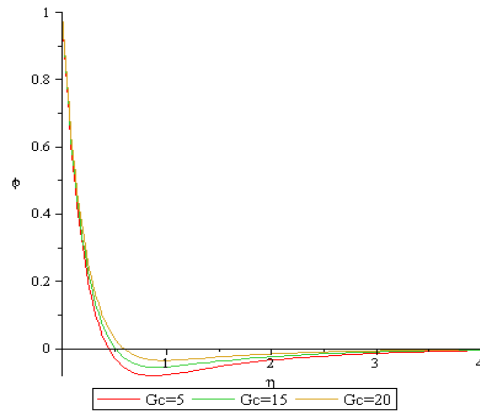
(a)

(b)

Figure 4. variation of Concentration Grashof number on velocity, temperature and concentration profiles

Figures 3 shows the variation of thermal Grashof number on velocity (a) and temperature profile (b). The velocity and temperature profile of the fluid increases with an increase in the thermal Grashof number due to the presence of buoyancy effects. It was also observed that the effects of buoyancy is more pronounced in the region far from the moving plane in the temperature profile.

Figures 4 depicts the variation of concentration Grashof number on velocity (a), temperature profile (b) and concentration profile (c). The velocity, temperature and concentration profile of the fluid raises as the concentration Grashof number rose which is due to the buoyancy effect. The rate of increase in the velocity and temperature profile with increase in concentration Grashof number is low.
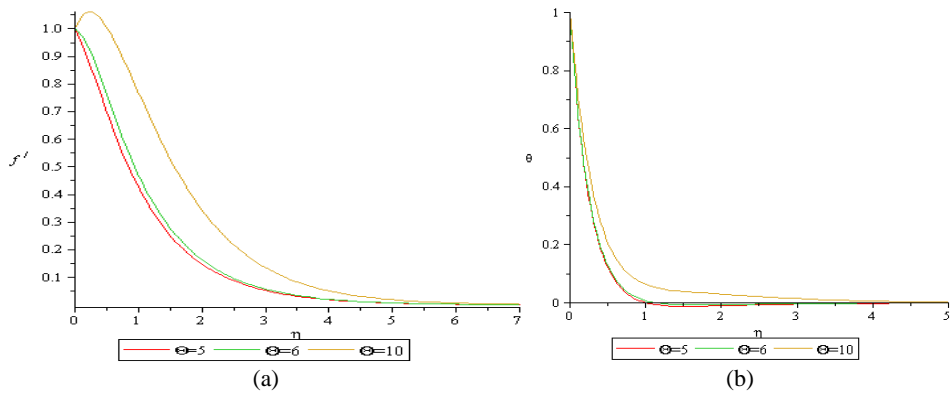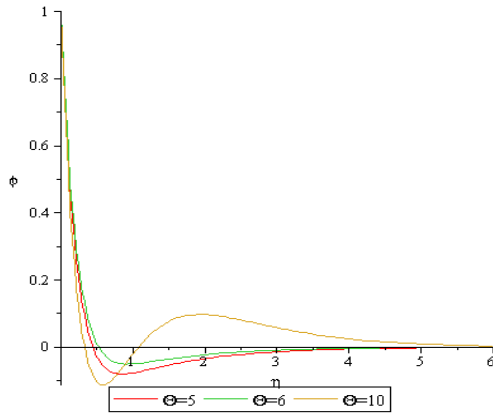
(a)

(b)

Figure 5. Variation of angle of inclination on velocity, temperature and concentration profiles

(a) (b)
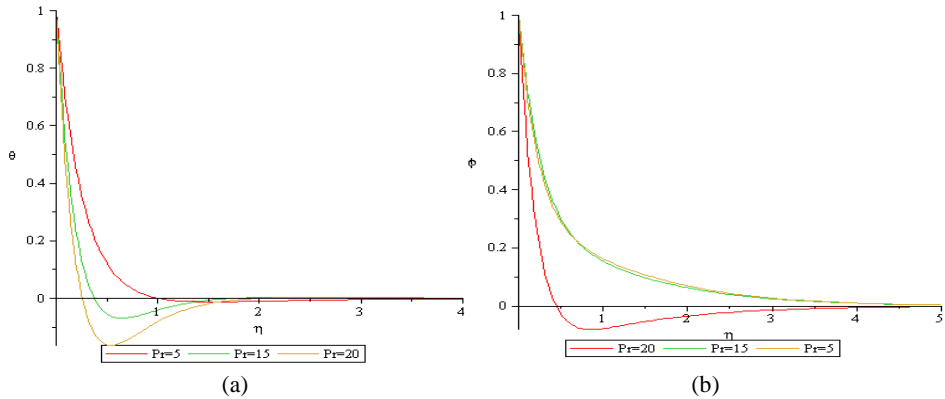
Figure 6. Variation of Prandtl number on temperature and concentration profile
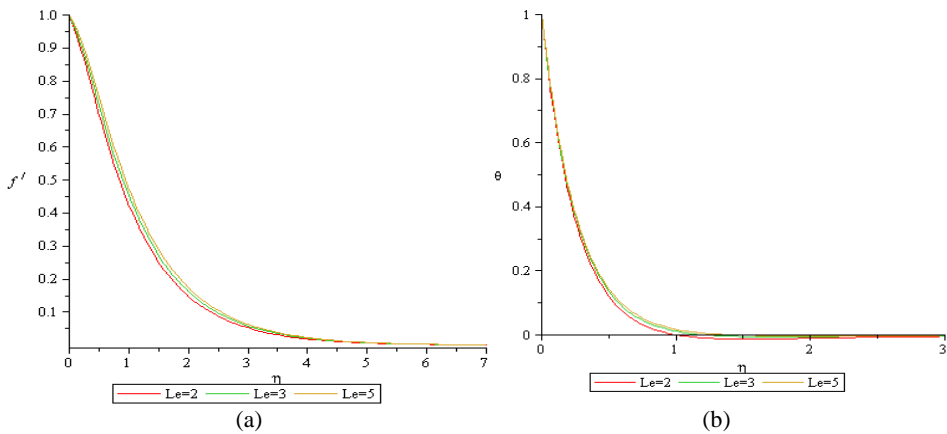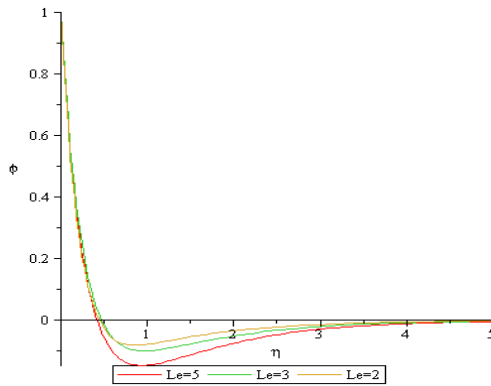
(a) (b)

(a)

Figure 7. Variation of Lewis number on velocity, temperature and concentration profiles

(a)

(b)

(c)

Figure 8. Variation of thermopheric parameter on the velocity, temperature and concentration profiles

Table 1. Comparison of Skin Friction $\left(-f^{//} \right)$

M	NM	ADM
0.1	1.0519	1.0488
0.2	1.0977	1.0955
0.3	1.1402	1.1418
0.4	1.1844	1.1832
0.5	1.2256	1.2248
0.6	1.2655	1.2649
0.8	1.3419	1.3416
1	1.4144	1.4142

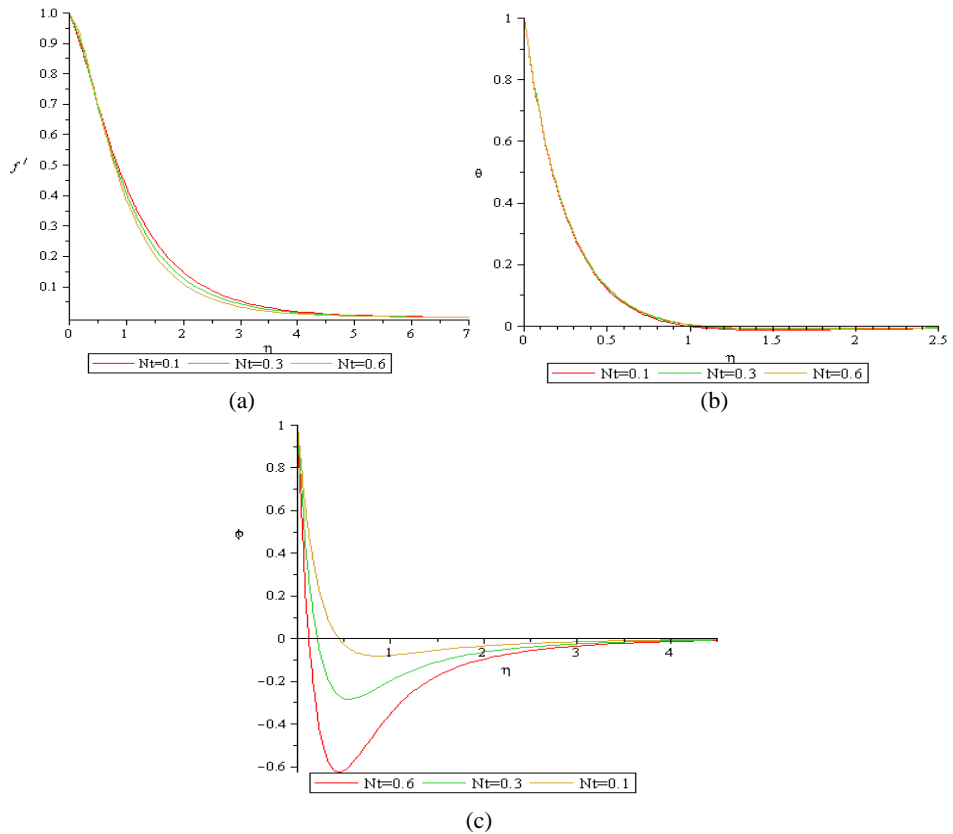Figures 5 present variation of angle of inclination on velocity, temperature and concentration profile of the fluid. The fluid velocity is enhanced as the angle increases due to the presence of gravity and since the flow is in favour of it. At a very high value of angle of inclination the fluid velocity at the wall rises before it finally dropped and the concentration has the tendency to behave sinusoidal. It is also observed that temperature and concentration are also enhanced with the angle of inclination.

Figures 6 is the variation of Prandtl number on the fluid temperature (a) and concentration profile (b). As Prandtl number increases, both temperature boundary layer of the fluid and the concentration dropped. This shows that at a very high value of Prandtl number, heat is able to diffuse out of the system.

Figures 7 show the effects of Lewis number on the velocity (a), temperature (b) and concentration (c) boundary layer. This parameter enhances the fluid velocity boundary layer and temperature, but the concentration boundary layer is reduced. The rate of increase in the temperature is very low.

Figures 8 show the effects of thermopheris parameter on the velocity (a), temperature (b) and concentration (c) boundary layer. Increase in this parameter dropped the fluid velocity boundary layer and concentration as the fluid moves far from the plane, but has an insignificant effect on the temperature boundary layer. It is also observed that there is no significant effect of this parameter in the region closer to the wall on the velocity profile.

5. CONCLUSION

The problem of laminar flow in an inclined stretching sheet has been considered in 2-dimension with magnetic field effect *(M)* without convective heating. The local similarity solution were obtained and solved using the improved ADM and the analytical solution were presented which depends on magnetic parameter *(M)*, thermal and concentration Grashof number (Gr and Gc respectively), Lewis number, and Prandtl number. It was found that:-

1. All the graphs presented in this work clearly obey the boundary conditions.
2. A negative temperature was observed at a very high Prandtl number.
3. The analytical result presented in this work gives a solution at every point unlike the numerical results presented by Makinde and Aziz (2011) which only give results at mesh points.
4. The flow velocity is in favour of gravity.
5. The method is in good agreement with numerical method which further enhances the integrity of the Adomian Decomposition Method in handling nonlinear coupled differential equations.
6. This work, if implemented will serve as a guide to industrialists that specialises in the development of high thermal conductivity fluid as to how each of the physical property influences the fluid velocity, temperature and concentration profile.

REFERENCES

[1]   Abu-Nada, E., Masoud, F., Oztop, H. F. & Campo, A. (2010). Effect of nanofluid variable properties on natural convection in enclosures. *Int. J. of Therm. Sci.*, 49, 479-491.

[2]   Altan, T., Oh, S., & Gegel, H., (1979). Metal Forming Fundamentals and Applications. American Soc. of Met., Metals Park, OH.

[3]   Ayub, M., Abbas, T., and Bhatti, M. M. (2016). Inspiration of slip effects on electromagnetohydrodynamics (EMHD) nanofluid flow through a horizontal Riga plate. Eur. Phys. J. Plus 131, 193.

[4]   Bhatti, M.M. and Rashidi, M. M. (2016). Effects of thermo-diffusion and thermal radiation on Williamson nanofluid over a porous shrinking/stretching sheet. *J. of Mol. Liq.* 221, 567–573.

[5]   Bhatti, M. M., Abbas, M. A., and Rashidi, M. M. (2018). A robust numerical method for solving stagnation point flow over a permeable shrinking sheet under the influence of MHD. App. Math. and Comp. 316, 381–389.

[6]   Beg, O. A., Rashidi, M. M., Akbari, M. ,& Hosseini, A. (2014). Comparative numerical study of single-phase and two-phase models for bio-nanofluid transport phenomena. *J. of Mech. in Med. and Bio.*, 14. DOI: 10.1142/S0219519414500110.

[7]   Hassan, M., Faisal, A. and Bhatti, M. M. (2018). Interaction of aluminum oxide nanoparticles with flow of polyvinyl alcohol solutions base nanofluids over a wedge. App. Nano sci. 8, 53–60.

[8]   Makinde, O. D., & Aziz A., (2011). Boundary layer flow of a nanofluid past a stretching sheet with a convective boundary condition. *Int. J. of Therm. Sci.* 50, 1326-1332.

[9]   Mustafa, M., Hayat, T., Pop, I., Asghar, S., & Obaidat, S. (2011). Stagnation-point flow of a nanofluid towards a stretching sheet. *Int. J. of Heat and Mass Trans.* 54, 5588-5594.

[10]   Prasad, K. V.,Vajravelu, K., & Dutt, P. S., (2010). The effects of variable fluid properties on the hydro-magnetic flow and heat transfer over a non-linearly stretching sheet, Int. J. Therm. Sci. 40, 603-610.

[11]   Qing, J., Bhatti, M. M., Abbas, M. A., Rashidi, M. M. and Ali, M.E. (2016). Entropy Generation on MHD Casson Nanofluid Flow over a Porous Stretching/Shrinking Surface. Entropy, 18, 123.

[12]   Rashidi, M. M., Hosseini, A., Pop, I., Kumar, S., & Freidoonimehr, N. (2014). Comparative numerical study of single and two-phase models of nanofluid heat transfer in wavy channel. *App. Math. and Mech.* 35, 831-848.

[13]   Rashidi, M. M., Abelman, S., & Freidoonimehr, N. (2013). Entropy generation in steady magnetohydrodynamic flow due to a rotating porous disk in a nanofluid. *Int. J. of Heat and Mass Trans.* 62, 515-525.

[14]   Yusuf, A., Aiyesimi, Y.M., Jiya, M., Okedayo G. T. and Bolarin G. (2016). Analysis of Unsteady Hydromagnetic Boundary Layer Flow in an Inclined wavy Permeable wall of a Nanofluid with Soret and Dufour effects and Heat Generation with Convective Boundary Condition. *J. of Nig. Ass. of Math. Phys. 36* (1), 125-134.

[15]   Yusuf, A., Bolarin G., Jiya, M., Aiyesimi, Y.M., and Okedayo G. T. (2018). Boundary layer flow of a nanofluid in an inclined wavy wall with convective boundary condition. *Comm. in Math. Mod. and App. 3* (2), 48-56.

[16]   Yusuf, A., Bolarin G. and Adekunle, S. T. (2019). Analytical solution of unsteady boundary layer flow of a nanofluid past a stretching sheet with effects of magnetic field. *FUOYE J. of Eng. and Tech. (FUOYEJET), in press.*